Pyrochemical Electrorefining Behaviors of Co and Ni in LiCl-KCl Eutectic Salts for Decontamination of PWR In-core Stainless Steel

Jungho Hur*, Sungjune Sohn, Seongjin Jeong and Il Soon Hwang
Department of Energy System Engineering, Seoul National University,
One Gwanak-ro, Gwanak-gu, Seoul, 08826, Republic of Korea
**Corresponding author: jhhur@snu.ac.kr*

1. Introduction

Austenitic stainless steels have been widely used for reactor vessel internals. During the operation of nuclear power plants, reactor vessel internals get contaminated by primary coolant system (surface contamination) and neutron activation (volumetric contamination). For surface contamination, to eliminate radioactive elements on the internal surface of reactor vessels during decommissioning phases, various surface decontamination methods such as chemical agents are being used. For Volumetric contamination of reactor internals in high neutron flux region, there is no effective method for the elimination. Among these contaminated parts, including baffle, former, barrel, and thermal shield, which are classified as intermediate level wastes with long living radioactive elements (C-14, Nb-94, Ni-59, Ni-63) and Co-60, are being stored in storage in most countries. Even though low-intermediate level waste repository in Gyeongju is being operated, long-living intermediate level wastes cannot be disposed to Gyeongju repository in current regulation as well. Reprocessing or volume reduction of these wastes is necessary not only to meet the current regulation but to manage repository efficiently for the long term management perspective. Currently, pyrochemical method which makes less secondary wastes than other ways is considered as one of the most appropriate decontamination method. Therefore, to develop the process, electrokinetic properties of elements from stainless steels in LiCl-KCl eutectic salt at 500℃ were investigated in the present study.

2. Experimental

Electrochemical experimental setup was built in a glove box filled and continually purged with Argon gas (Purity: 99.999 wt. %). Oxygen and moisture contents were maintained lower than 0.1ppm. A proportional-integral-derivative (PID) controller was installed for furnace that were located at the bottom well of the glove box. Electrochemical measurement systems are controlled by a VersaStat3 potentiostat and VersaStudio software.

A LiCl-KCl eutectic salt with purity of 99.99 wt. % and $CoCl_2$ and $NiCl_2$ with purity of 99.9 wt. % were supplied from Sigma Aldrich. All reagents were open and handled in a glove box. AgCl with the purity of 99.999 wt. % and Tungsten and Ag wires for electrodes were supplied from Sigma Aldrich.

Quartz cell with an inner diameter of 11mm was located in the furnace and three electrodes were put in the quartz cell. Two tungsten wires for working electrode and counter electrode were guided by a quartz tube with an inner diameter of 2mm. The 1cm tip of tungsten wires were dipped in molten salt and contacted area was 0.628cm^2. A Ag wire with 99.99% purity for reference electrode was immersed in Pyrex tube containing LiCl-KCl with 1 wt. % AgCl. The temperature in a quartz cell was kept at 500±1℃ and monitored by a Type-K thermocouple in identical quartz tube attached outer surface of the main cell.

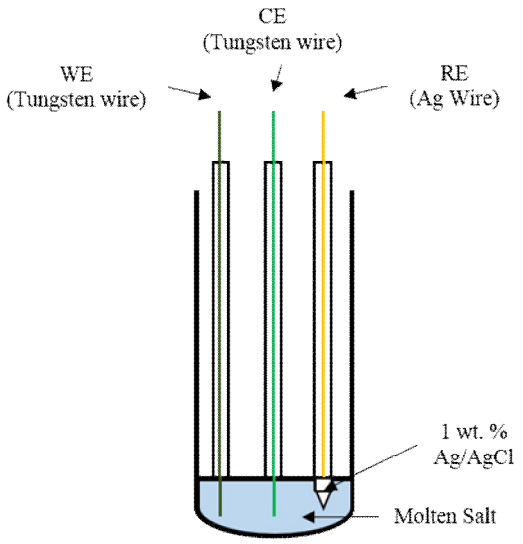

Fig. 1. Schematic of electrochemical cell for cyclic voltammetry.

Test matrix of Cyclic Voltammetry (CV) in this study is summarized in Table I.

Table I: Test matrix of Cyclic Voltammetry

Molten Salt	Concentration (wt. %)	Scan range (V vs. 1 wt. % Ag/AgCl)	Scan rate (mV/s)
LiCl-KCl-$CoCl_2$	0.1	-1~0.4	- 30 - 50 - 100 - 150 - 200
LiCl-KCl-$NiCl_2$			

3. Results and Discussions

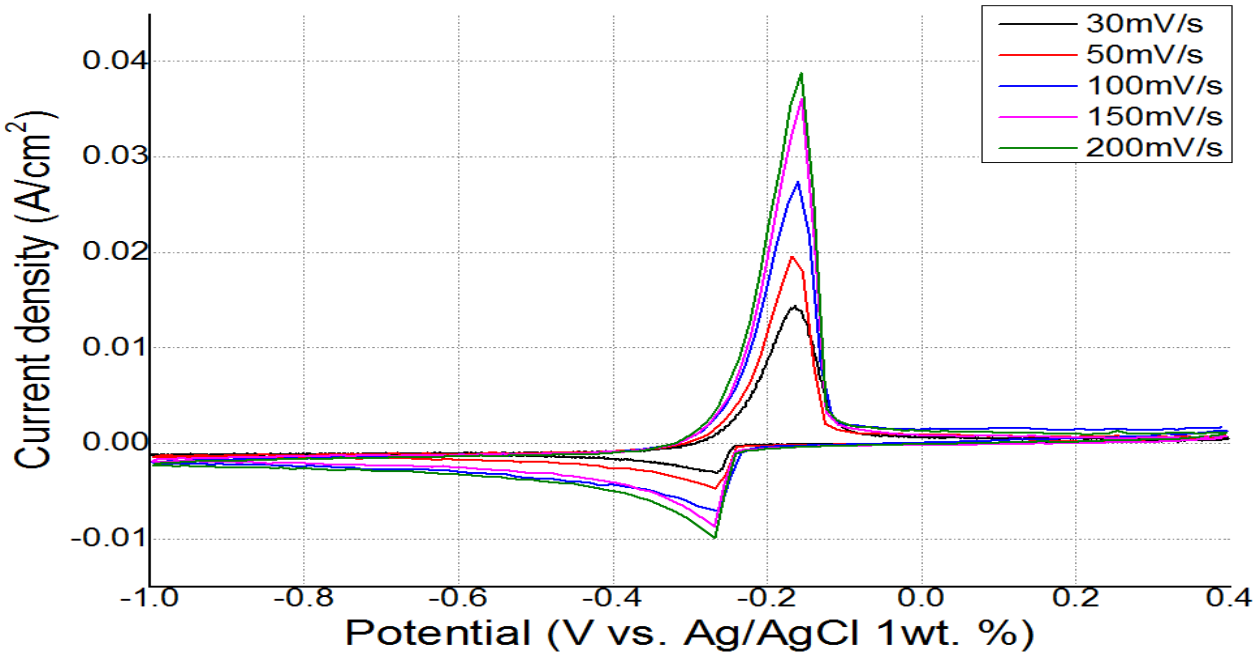

(a)

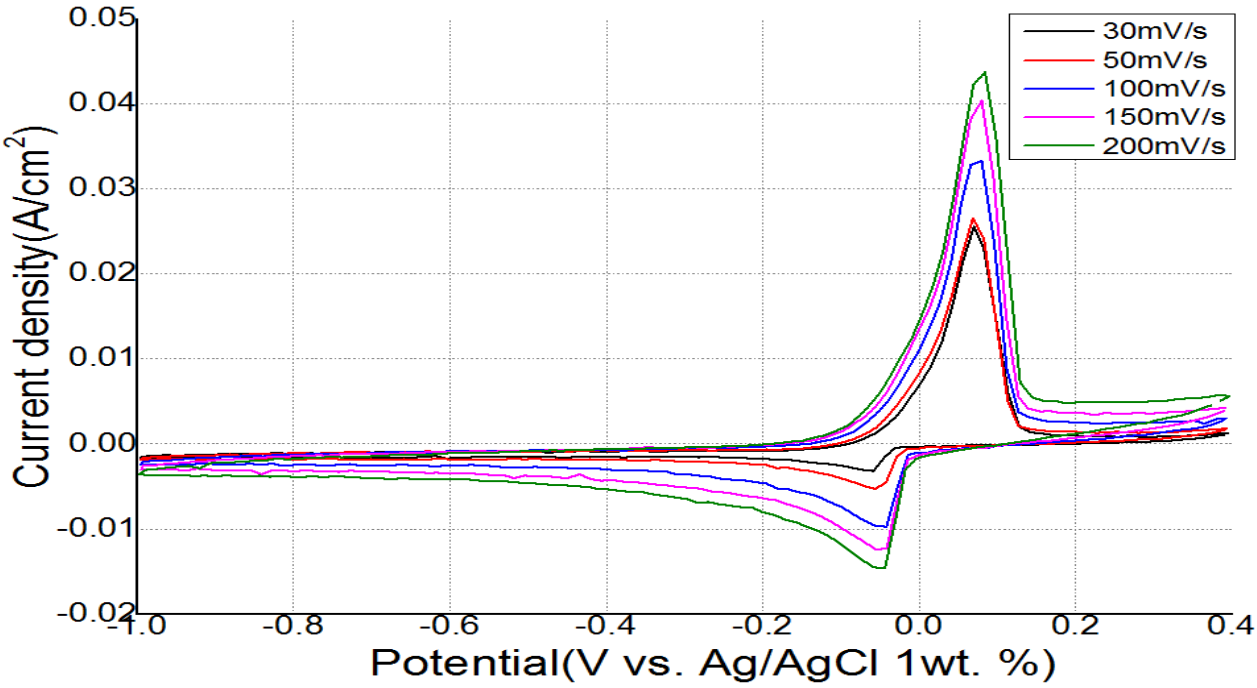

Fig. 2. Cyclic voltammogram for (a) Co^{2+} and (b) Ni^{2+} in LiCl-KCl eutectic salt at 500℃

3.1. Redox behavior of Co and Ni in LiCl-KCl eutectic salt at 500 ℃

Two cyclic voltammograms are presented in Fig. 2. In Agreement with earlier studies [1,2], single reduction and oxidation peak pair was observed in both $CoCl_2$ and $NiCl_2$. Co^{2+} and Ni^{2+} have very similar redox behavior in LiCl-KCl molten salt. They have single soluble state in LiCl-KCl and reduction of Ni^{2+} to Ni occur at small higher potential (about 0.2 V) than Co^{2+}.

3.2. Electrokinetic properties of Fe, Co and Ni in LiCl-KCl eutectic salt

3.2.1. Apparent reduction potential

Apparent reduction potentials of both Co^{2+} and Ni^{2+} in LiCl-KCl at 500℃ was estimated using following Nernst equation:

$$E^{0'} = E_p - \frac{RT}{nF} lnX_{M^{n+}} - 0.854\frac{RT}{nF} + E^0_{AgCl} + \frac{RT}{F} lnX_{AgCl} \quad (1)$$

where $E^{0'}$ is the apparent reduction potential (V), E_p is the peak potential (V), R is the gas constant (8.314 J/mol-K), T is the temperature (K), n is the number of electrons, F is the Faraday constant(96,485 C/mol), and X_{Mn+} is the mole fraction of M^{n+}. The standard reduction potential of Ag (-0.853 V vs. Cl_2/Cl^- reported by Iizuka et al.[3]) was used to convert the measured potentials from Ag/AgCl reference to Cl_2/Cl^-. Table II. shows the results of apparent reduction potential and comparison with standard reduction potential.

Table II: Apparent standard reduction potential comparison on Co^{2+} and Ni^{2+} in LiCl-KCl eutectic salt at 500℃.

Current study				Iizuka et al. (V vs. Cl_2/Cl^-) [3]
	Apparent reduction potential (V vs. Cl_2/Cl^-)			
	Avg.	Min (scan rate)	Max (scan rate)	
Co^{2+}/Co	-1.279	-1.282 (0.05V/s)	-1.275 (0.03V/s)	-1.207
Ni^{2+}/Ni	-1.064	-1.073 (0.03V/s)	-1.058 (0.1V/s)	-1.011

3.2.2. Diffusion coefficient

The diffusion coefficients of Co^{2+} and Ni^{2+} were assessed using cathodic peak current variation with the square root of scan rates. Cathodic peak currents are plotted as the changes of the square root of scan rates and linear fitting lines are drawn in Fig 3. It was calculated based on the Berzins-Delahay equation for a reversible electrodeposition.

$$i_p = 1.082nFAC\sqrt{\frac{nFDv}{RT\pi}} \quad (2)$$

where i_p is the peak current (V), A is the electrode area (cm^2), D is diffusion coefficient (m^2/s), and v is scan rate (V/s).

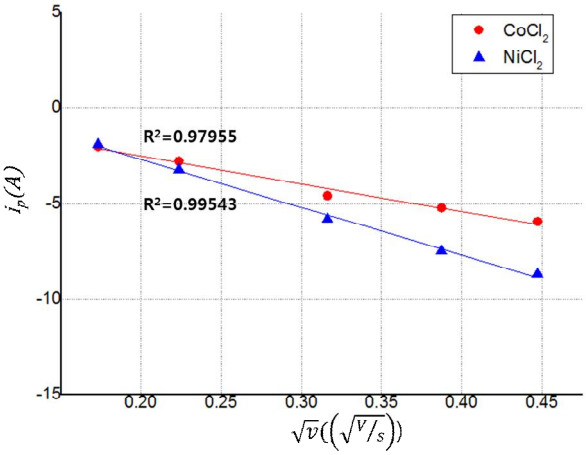

Fig. 3. Cathodic peak current variation of Co^{2+} and Ni^{2+} with the square root of scan rates in LiCl-KCl eutectic salt at 500℃.

Calculated diffusion coefficients are presented and compared to reported values in Table III. The diffusion coefficient of Co^{2+} reported by J. Park et al.[1] is 1.16 x $10^{-9}m^2/s$ and the value for Ni^{2+} reported by D. Yamada et al.[4] is1.5 x 10-9m^2/s.

Table III: Diffusion coefficient comparison on Co^{2+} and Ni^{2+} in LiCl-KCl eutectic salt at 500℃.

Current study				Earlier Results [1,4]
	Diffusion coefficient (m^2/sec)			
	Avg.	Min (scan rate)	Max (scan rate)	
Co^{2+}/Co	$5.64 \cdot 10^{-10}$	$4.48 \cdot 10^{-10}$ (0.03V/s)	$6.84 \cdot 10^{-10}$ (0.1V/s)	$1.16 \cdot 10^{-9}$ [1]
Ni^{2+}/Ni	$9.46 \cdot 10^{-10}$	$4.13 \cdot 10^{-10}$ (0.03V/s)	$1.25 \cdot 10^{-9}$ (0.2V/s)	$1.5 \cdot 10^{-9}$ [5]

3.2.3. Exchange current density and Charge transfer coefficient

For Tafel method, linear polarization method and electrochemical impedance spectroscopy (EIS) are generally used to calculate the exchange current density. Among those methods, tafel method can estimate both exchange current density and charge transfer coefficient.

Butler-Volmer equation is describing the charge transfer kinetics of soluble-insoluble process.

$$i = i_0\left[exp\left(\frac{\alpha nF}{RT}\eta\right) - exp\left(-\frac{(1-\alpha)nF}{RT}\eta\right)\right] \quad (3)$$

where i is the current density (A/cm^2), i_0 is the exchange current density (A/cm^2), α is the charge transfer coefficient and η is the overpotential (V).

For sufficient overpotential, Eq. 3 can be simplified to

$$\ln(i) = ln(i_0) - \frac{\alpha nF}{RT}\eta \quad (4)$$

Thus, when linear fitting is applied to sufficient overpotential region, slope and intersection of fitting can be utilized to calculate exchange current density and charge transfer coefficient.

Fig. 4 shows the Tafel plots for both Co^{2+} and Ni^{2+} cases, where linear Tafel region from -0.2V to -0.1V and that from -0.4V to -0.2V can be found. Each linear regression data was obtained to calculate exchange current density and charge transfer coefficient (see Table IV).

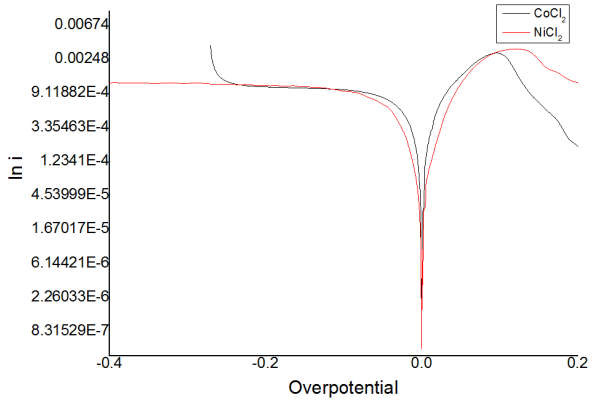

Fig. 4. Tafel plots of Co^{2+} and Ni^{2+} in LiCl-KCl eutectic salt at 500℃.

Table IV: Tafel region range and value of exchange current density and charge transfer coefficient in LiCl-KCl at 500℃.

	Tafel linear region (V)	**i_0 (A/cm^2)**	**α**
Co^{2+}/Co	-0.2~-0.1	$(9.51\pm0.23)\cdot10^{-4}$	0.029±0.007
Ni^{2+}/Ni	-0.4~-0.2	$(1.06\pm0.003)\cdot10^{-3}$	0.012±0.0004

4. Conclusions and Future Work

In the present study, electrokinetic parameters were obtained from cyclic voltammetry and Tafel methods as fundamental study for the development of pyrochemical decontamination method of irradiated reactor vessel internals. Cyclic voltammetry was applied to 0.1wt. % $CoCl_2$ and $NiCl_2$ to investigate redox behaviors in LiCl-KCl eutectic salt at 500℃ with scan range from -1 V to 0.4 V (vs. 1 wt. % Ag/AgCl) and five different scan rates (30, 50, 100, 150, 200mV/s). The results show that single redox peak pair was observed in both cases and they are reversible. Apparent reduction potentials and diffusion coefficients are calculated using reversible equations. Apparent reduction potentials of Co^{2+} and Ni^{2+} are -1.279 V and -1.064 V (vs. Cl^2/Cl^-), respectively. Diffusion coefficients of Co^{2+} and Ni^{2+} are $5.64 \cdot 10^{-10} m^2/sec$ and $9.46 \cdot 10^{-10} m^2/sec$, respectively. Using Tafel methods, exchange current densities and charge transfer coefficients are also calculated. Exchange current densities of Co^{2+} and Ni^{2+} are $(9.51\pm0.23)\cdot10^{-4}$ A/cm^2 and $(1.06\pm0.003)\cdot10^{-3}$ A/cm^2. Charge transfer coefficients of Co^{2+} and Ni^{2+} are 0.029±0.007 and 0.012±0.0004 in order.

Electrochemical behavior study on rich elements (i.e. Fe and Cr) of irradiated stainless steel is also being investigated in same experimental condition. As the follow-up study, coexistence case that small and large concentrated elements in irradiated austenitic stainless steel Type 304 will be studied. Additionally, radioactivity distribution analysis on irradiated reactor vessel internals will be investigated by using Monte Carlo Code for Advanced Reactor Design and Analysis (McCARD). Then, decontamination process for PWR in-core stainless steel will be designed and optimized.

REFERENCES

[1] J. Park, S. Choi, S. Sohn, and I. S. Hwang, Cyclic Voltammetry on Zr, Sn, Fe, Cr and Co in LiCl-KCl Salts at 500℃ for Electrorefining of Irradiated Zircaloy-4 Cladding, Journal of The Electrochemical Society, Vol. 164, No. 12, pp.744-751, 2017.

[2] Pyeong-Hwa Kim, A Study on Electrochemical Decontamination of Irradiated Zr-Nb Alloys in LiCl-KCl Eutectic Molten Salts, Master dissertation, 2016.

[3] M. Iizuka, T. Inoue, O. Shirai, T. Iwai, and Y. Arai, Application of normal pulse voltammetry to on-line monitoring of actinide concentrations in molten salt electrolyte, Journal of nuclear materials, Vol. 297, pp.43-51, 2001.

[4] D. Yamada, T. Murai, K. Moritani, T. Sasaki, I. Takagi, H. Moriyama, K. Kinoshita, H. Yamana, J. Alloys Compd. 444-445 (2007) 557-560.

[5] Sungjune Sohn, Intermetallic Density Based Group Separation of Actinides and Lanthanides Using Liquid Bi to Decontaminate High Level Wastes from Pyroprocessing, Doctoral dissertation, 2018.